Applied Catalysis A: General 491 (2015) 106–115

Contents lists available at ScienceDirect

Applied Catalysis A: General

journal homepage: www.elsevier.com/locate/apcata

Reusable chiral salen Mn(III) complexes with phase transfer capability efficiently catalyze the asymmetric epoxidation of unfunctionalized olefins with NaClO

Yaju Chen[a], Rong Tan[a,*], Yaoyao Zhang[a], Guangwu Zhao[a], Weiguo Zheng[a], Rongchang Luo[a], Donghong Yin[a,b,**]

[a] Institute of Fine Catalysis and Synthesis, Key Laboratory of Chemical Biology and Traditional Chinese Medicine Research (Ministry of Education), Hunan Normal University, Changsha, Hunan 410081, China
[b] Technology Center, China Tobacco Hunan Industrial Corporation, NO. 426 Laodong Road, Changsha, Hunan 410014, China

ARTICLE INFO

Article history:
Received 26 August 2014
Received in revised form
26 November 2014
Accepted 30 November 2014
Available online 9 December 2014

Keywords:
Chiral salen Mn(III) complex
Phase transfer catalysis
Enantioselective epoxidation
Unfunctionalized olefins
Aqueous/organic biphasic system

ABSTRACT

A series of chiral salen Mn(III) polymers with build-in phase transfer capability was prepared by bridging the chiral salen Mn(III) units with polyethylene glycol (PEG)-based di-imidazolium ionic liquid (IL) side by side. Technologies of characterization suggested the alternation of intact chiral salen Mn(III) unit with PEG-based dicationic imidazolium IL moiety in the rigid one-dimension polymers. Amphipathic nature of PEG-based di-imidazolium IL moiety allowed the obtained catalysts to undergo inherent phase transfer catalysis in asymmetric epoxidation of unfunctionalized olefins with NaClO, which in turn increased the reaction rate of epoxidation in water–dichloromethane biphasic system. Decreasing total length of polyether chain leads to an increase in built-in phase transfer capability of corresponding complex, which further enhances the catalytic performance. 91–97% of conversion was obtained in the enantioselective epoxidation of styrene, α-methylstyrene, indene, 1,2-dihydronaphthalene, 6-cyano-2,2-dimethylchromene, and 6-nitro-2,2-dimethylchromene catalyzed by the complex where number of ethylene oxide unit is 3 within 60 min, which is significant higher than that observed for the neat complex (56–74%) and the ICP (62–85%). High enantiomeric excess (ee) for the epoxides (in the range of 67–93%) was also achieved, except for styrene (ee, 34%) and α-methylstyrene (ee, 41%). Furthermore, the efficient phase transfer catalysts could be easily recovered by solvent precipitation and be recycled for seven times without significant loss of the activity and enantioselectivity.

1. Introduction

Optically active epoxides are key intermediates in organic chemistry because they can undergo stereospecific ring-opening reactions or functional group transformations, giving rise to a wide variety of biologically or pharmaceutically important compounds [1–3]. Enantioselective epoxidation catalyzed by chiral salen Mn(III) complex is one of the most efficient strategies for obtaining enantiopure epoxides [4–14]. Aqueous NaClO (*aq.* NaClO) is an attractive oxygen source for the transformation, since it is reasonably stable, readily available and environment friendly. Some pioneering contributions to the employment are known in the field of asymmetric epoxidation [15–19]. For example, Kureshy et al. have reported the catalytic asymmetric epoxidation of nonfunctionalized alkenes in dichloromethane catalyzed by dimeric or polymeric chiral salen Mn(III) complexes using *aq.* NaClO as an oxidant. The biphasic systems provided high activity (>99% of conversion) and enantioselectivity (in the range of 33–93%), but often require long reaction time (6–24 h) due to the limited mass transfer [15,18]. The reaction rate can be speeded up by using phase transfer catalysts (PTC) that improves the compatibility of aqueous/organic biphasic system [5]. Amphiphilic groups, such as tertiary amino alkyl groups [20] or phosphonium groups [21] have thus been introduced into the 5- and/or 5′-positions of chiral salen ligand to achieve the chiral salen Mn(III) complex with built-in phase transfer capability. Excellent catalytic performance regarding yield (99% of conversion) and enantioselectivity (in the range of 36–99% ee

---

* Corresponding author. Tel.: +86 731 8872576; fax: +86 731 8872531.
** Corresponding author at: Institute of Fine Catalysis and Synthesis, Key Laboratory of Chemical Biology and Traditional Chinese Medicine Research (Ministry of Education), Hunan Normal University, Changsha, Hunan, 410081, China.
Fax: +86 731 8872531.
E-mail addresses: yiyangtanrong@126.com (R. Tan), yindh@hunnu.edu.cn (D. Yin).

http://dx.doi.org/10.1016/j.apcata.2014.11.043
0926-860X/

value) was indeed obtained over the PTC in asymmetric epoxidation of unfunctionalized olefins with NaClO. Unfortunately, recovery and reuse of PTC from reaction mixture are often troublesome.

PEG with low molecular weight has emerged as the alternative modifier to develop the PTC of chiral salen Mn(III) complex for water/oil biphasic systems, not only due to the phase transfer capability, but also because the selective solubility profile of PEG may facilitate the recovery of catalyst through solvent precipitation [22–24]. Recently, we have reported a series of chiral salen Mn(III) complexes functionalized by PEG-modified imidazolium IL (PEG-IL) moiety for the enantioselective epoxidation of unfunctionalized olefins with NaClO [25]. Remarkable enhancement of reaction rate was observed over the catalysts in the biphasic system due to the built-in phase transfer capacity originated from the amphiphilic PEG chain, as well as the positive effect of the imidazolium based-IL moieties. However, leaching loss of catalyst was also inevitable due to the amphiphilic nature of complex, although PEG-IL modifier potentially enabled the separation of catalysts by changing solvent. Interestingly, reduced leaching was observed over the catalyst which contains more number of ethylene glycol units. The facts encouraged us to anticipate that properly increasing the molecular weight of catalyst would lower its solubility, aiding catalyst recovery. Previous report shows that increasing the number of active sites for catalyst results in higher reactivity and turnover [26,27]. Therefore, it is desirable to use the PEG-IL and chiral salen Mn(III) complex as building blocks to fabricate polymeric analog for the biphasic system. We envisaged that the polymeric chiral salen Mn(III) catalyst containing PEG-IL moiety would not only behave as a PTC in the aqueous/organic biphasic system, but also could be facilely recovered from reaction system for efficient reuse.

Herein, PEG-bridged di-imidazole was synthesized and N-alkylated with the chiral salen Mn(III) complex of [(*R*,*R*′)-(N,N′-bis(3-*tert*-butyl-5-chloromethyl salicylidene)-1,2-cyclohexanediaminato] manganese(III) chloride. The successful N-alkylation gave the PEG-IL functionalized chiral salen Mn(III) polymers (**PICP**), in which chiral salen Mn(III) units were bridged by PEG-based di-imidazolium IL side by side. It has proved that the catalysts could achieve the process of phase transfer catalysis in asymmetric epoxidation of unfunctionalized olefins using NaClO as an oxidant. Remarkable enhancement of reaction rate with high turnover frequency (TOF) values was observed over a wide range of alkenes. More importantly, the catalysts could be quantitatively recovered from the reaction mixture by solvent precipitation for efficient reuse. Thus, the problems associated with phase transfer limitation in the water–oil biphasic reaction and the separation of catalyst can be well resolved. In addition, the total length of polyether chain significantly affected the phase transfer capability, and further affected the catalytic performance of **PICP** in the water–dichloromethane biphasic system.

2. Experimental

2.1. Materials and reagents

L-(+)-Tartaric acid (>99% ee) and (±)-1,2-diaminocyclohexane (purity, 99%) were purchased from Alfa Aesar. *Pyridine N-oxide* (purity, 98%) was bought from Aldrich. Indene (purity, >99%) and 1,2-dihydronaphthalene (purity, >99%) were obtained by TCI. Other commercially available chemicals were laboratory grade reagents from local suppliers. All solvents were purified by standard procedures. Styrene and indene were passed through a pad of neutral alumina before use. Chloride-terminated PEG was prepared according to the reported procedures [28]. 6-Cyano-2,2-dimethylchromene and 6-nitro-2,2-dimethylchromene were synthesized according to the literature procedures [29]. Neat complex of [(*R*,*R*′)-(N,N′-bis(3,5-di-*tert*-butylsalicylidene)-1,2-cyclohexanediaminato] manganese(III) chloride was prepared according to the described procedures [30]. The chiral salen Mn(III) complex of [(*R*,*R*′)-(N,N′-bis(3-*tert*-butyl-5-chloromethyl salicylidene)-1,2-cyclohexane diaminato]manganese(III) chloride was synthesized by a previously described procedure [31].

2.2. Methods

FT-IR spectra were obtained as potassium bromide pellets with a resolution of 4 cm^{-1} and 32 scans in the range 400–4000 cm^{-1} using an AVATAR 370 Thermo Nicolet spectrophotometer. The sample concentration used for pellet preparation is ca. 1 wt%. The ultraviolet–visible light (UV–vis) spectra were recorded on a UV–vis Agilent 8453 spectrophotometer. The solution of samples in dichloromethane (ca. 1.0 mM) was poured into a 1 cm quartz cell for UV–vis spectroscopy with dichloromethane as the reference. The termogravimetric and differential thermogravimetric (TG-DTG) curves were obtained on a NETZSCH STA 449C thermal analyzer. Samples were heated from room temperature up to 700 °C under flowing air using alumina sample holders. The sample weight was ca. 10 mg and the heating rate was 10 K/min. ^1H NMR spectra of samples were recorded on a Varian-500 spectrometer with TMS as an internal standard. Thin layer chromatography (TLC) was conducted on glass plates coated with silica gel GF_{254}. Mn ion contents were measured by the method of complexometry with ethylenediamine tetraacetic acid (EDTA) [32]. The molecular weight of catalysts was obtained by gel permeation chromatograph (GPC). Analyses were performed on an Alltech Instrument (Alltech, America) equipped with an Alltech ELSD 800 detector. Mass spectrometry analyses were performed using an API 3000 tandem mass spectrometer (Applied Biosystems, USA) with electrospray interface (ESI-MS/MS in methanol). The optical rotation of catalysts was measured in dichloromethane on a WZZ-2A Automatic Polarimeter. The conversions and the ee values were measured by a 6890 N gas chromatograph (Agilent Co.) equipped with the chiral capillary column (HP19091G-B213, 30 m × 0.32 mm × 0.25 μm) and the FID detector.

2.3. Preparation of PICP-n (n = 3, 8, 12) (where n is the average numbers of ethylene oxide unit in various PEG chains)

The preparation of **PICP-*n*** ($n = 3, 8, 12$) was outlined in Scheme 1.

2.3.1. Synthesis of PEG-bridged di-imidazole

Sodium ethylate (0.68 g, 10 mmol) in anhydrous ethanol (10 ml) was dropwise added into the anhydrous ethanol solution (20 ml) of imidazole (0.68 g, 10 mmol). The resulting mixture was stirred at 60 °C for 8 h. Chloride-terminated PEG-*n* (5 mmol, $n = 3, 8, 12$, which is the corresponding average numbers of ethylene oxide unit in the PEG chains of PEG-200, PEG-400 and PEG-600) was then slowly added into the stirring mixture. The mixture was stirred at 70 °C for another 12 h, resulting in the formation of some white precipitate. After filtration, the filtrate was collected and concentrated in vacuum. The gummy residue was dissolved in dichloromethane (100 ml) and filtrated again to completely remove the insoluble salt of sodium chloride. The filtrate was washed with saturated sodium chloride and deionized water for several times. The organic phase was dried over anhydrous Na_2SO_4 and further dried at 40 °C in vacuum to obtain the sticky brownish red products of PEG-bridged di-imidazole. PEG-bridged di-imidazole ($n = 3$): ^1H NMR ($CDCl_3$, 500 MHz) δ_H, ppm: 7.47 (s, 2H, ring NC*H*N), 7.05 (s, 2H, ring C=NC*H*), 6.96 (s, 2H, ring N—C=CH), 4.13 (t, $J = 5.2$ Hz, 4H, $O—CH_2—CH_2—N_{ring}$), 3.72–3.76 (t, $J = 5.2$ Hz, 4H, $O—CH_2—CH_2—N_{ring}$), 3.54–3.72 (m, 8H, $CH_2—O—C_2H_4—O—CH_2$).

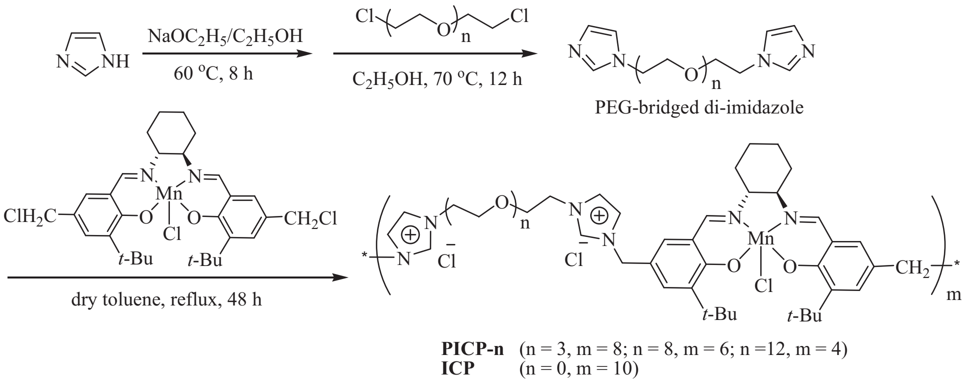

Scheme 1. Synthesis of **PICP-*n*** ($n = 3, 8, 12$) and **ICP**.

FT-IR (KBr): γ_{max}/cm^{-1} 2879, 1657, 1511, 1443, 1361, 1242, 1100, 945, 880, 831, 710, 667, 623.

2.3.2. Synthesis of ***PICP-n*** (*n* = 3, 8, 12)

[(*R,R*′)-(N,N′-bis(3-*tert*-butyl-5-chloro-methyl salicylidene)-1,2-cyclohexanediaminato] manganese(III) chloride (3.2 g, 5.1 mmol) was mixed with PEG-bridged di-imidazole (5 mmol) in dry toluene (20 ml). The mixture was refluxed for 48 h under nitrogen atmosphere. After removal of the solvent in vacuum, the mixture was washed with ether for several times. The gummy residue was dried in vacuum at 40 °C to provide **PICP-*n*** as the brown and viscous liquid (where *n* is the average numbers of ethylene oxide unit in various PEG chains, $n = 3, 8, 12$). The **PICP** containing the average numbers of ethylene oxide unit in PEG moiety of 3, 8 and 12 were denoted as **PICP-3**, **PICP-8** and **PICP-12**, respectively. **PICP-3**: FT-IR (KBr): γ_{max}/cm^{-1} 3125, 2948, 2865, 1618, 1543, 1439, 1386, 1339, 1309, 1266, 1235, 1205, 1164, 1100, 1066, 1039, 932, 866, 827, 783, 750, 661, 622, 571, 483, 416. UV–vis (CH_2Cl_2): 502 (2080), 406 (13,714), 317 (28,604) nm. Mn ion content: 0.814 mmol/g (theoretical value: 1.05 mmol/g); $\alpha_D{}^{28}$ = +619 (C = 0.02, CH_2Cl_2). The average molecular weight of the **PICP-3** is around 7600 g/mol ($M_W = 7600$, $m = 8$) based on GPC analysis; **PICP-8**: FT-IR (KBr): γ_{max}/cm^{-1} 3125, 2946, 2865, 1618, 1543, 1441, 1390, 1348, 1308, 1235, 1206, 1100, 1030, 933, 867, 828, 783, 774, 661, 622, 571, 486, 416. UV–vis (CH_2Cl_2): 502 (1921), 406 (12,489), 317 (29,397) nm. Mn ion content: 0.695 mmol/g (theoretical value: 0.866 mmol/g); $\alpha_D{}^{28}$ = +560 (C = 0.02, CH_2Cl_2). The average molecular weight of the **PICP-8** is around 6700 g/mol ($M_W = 6700$, $m = 6$) based on GPC analysis; **PICP-12**: FT-IR (KBr): γ_{max}/cm^{-1} 3123, 2950, 2867, 1618, 1543, 1440, 1388, 1350, 1308, 1264, 1237, 1205, 1100, 934, 829, 779, 662, 622, 571, 487, 416. UV–vis (CH_2Cl_2): 502 (2317), 406 (14,157), 317 (26,112) nm. Mn ion content: 0.575 mmol/g (theoretical value: 0.741 mmol/g); $\alpha_D{}^{28}$ = +632 (C = 0.02, CH_2Cl_2). The average molecular weight of the **PICP-12** is around 6100 g/mol ($M_W = 6100$, $m = 4$) based on GPC analysis.

2.4. Preparation of the PEG-free counterpart

For comparison, the polymeric analog of PEG-free counterpart, in which chiral salen Mn(III) unit alternates with ethyl-based dicationic IL, was also prepared according to a similar preparation procedure to that of **PICP-*n***, as shown in Scheme 1. During the procedure, 1,2-dichloroethane was used instead of the chloride-terminated PEG to bridge imidazole moiety through nucleophilic substitution. The obtained ethyl-bridged di-imidazole was readily N-alkylated with the chloromethyl groups (—CH_2Cl) at two sides of 5,5′-positions in (*R,R*′)-(N,N′-bis(3-*tert*-butyl-5-chloromethyl salicylidene)-1,2-cyclohexane diaminato] manganese(III) chloride, giving the imidazolium based IL functionalized chiral salen Mn(III) polymer (denoted as **ICP**). The structure of **ICP** is shown in Chart 1. FT-IR (KBr): γ_{max}/cm^{-1} 3125, 2952, 2864, 1618, 1543, 1439, 1388, 1342, 1311, 1266, 1232, 1206, 1162, 1095, 932, 868, 827, 777, 752, 710, 660, 622, 571, 476, 416. UV–vis (CH_2Cl_2): 502 (1240), 406 (9161), 317 (27,513) nm. Mn ion content: 0.983 mmol/g (theoretical value: 1.34 mmol/g); $\alpha_D{}^{28}$ = +607 (C = 0.02, CH_2Cl_2). The average molecular weight of **ICP** is around 7700 g/mol ($M_W = 7700$, $m = 10$) based on GPC analysis.

2.5. Catalyst testing

PICP-*n* (4 mol%, based on Mn ion content in **PICP-*n***), unfunctionalized alkenes (0.5 mmol) and pyridine *N*-oxide (0.095 g, 1 mmol) were added into dichloromethane (2 ml) under stirring. Buffered NaClO (1 mmol, pH = 11.5) as an oxidant was then added in four equal portions at 0 °C. The progress of epoxidation was monitored by GC. After the reaction, volatile solvents were evaporated under in a vacuum. **PICP-*n*** was precipitated out from reaction system by the addition of *n*-hexane (5 ml), washed with ether (3 × 5 ml), dried in vacuum, and finally recharged with fresh solvents and reaction substrates for the next catalytic cycle. Supernatant was decanted and separated by separatory funnel. Aqueous phase was extracted with CH_2Cl_2 for several times. The extract was combined with organic phase. The collected organic phase was dried over anhydrous sodium sulfate and concentrated in vacuum. Further purification of the residue by flash column chromatography afforded pure epoxides. The conversions and ee values were measured by a 6890 N gas chromatograph (Agilent Co.) equipped with a chiral capillary column (HP19091G-B213, 30 m × 0.32 mm × 0.25 μm) and a FID detector. Nitrogen was used as the carrier gas with a flow of 30 ml min^{-1}. The injector temperature is 250 °C, and the detector temperature is also 250 °C. The retention times of the corresponding chiral epoxides ($t_{absolute\ configuration}$) are as follows: (a) styrene epoxide: the column temperature is 90 °C, $t_R = 15.2$ min, $t_S = 15.7$ min; (b) α-methylstyrene epoxide: the column temperature is 80 °C, $t_S = 16.3$ min, $t_R = 16.5$ min; (c) indene epoxide: the column temperature was programmed from 80 to 180 °C with 8 °C min^{-1}, $t_{SR} = 11.5$ min, $t_{RS} = 11.9$ min; (d) 1,2-dihydronaphthalene epoxide: the column temperature was programmed from 80 to 180 °C with 6 °C min^{-1}, $t_{SR} = 13.4$ min, $t_{RS} = 13.6$ min; (e) 6-cyano-2,2′-dimethylchromene epoxide: the column temperature was programmed from 80 to 200 °C with 4 °C min^{-1}, $t_{SS} = 24.0$ min, $t_{RR} = 24.3$ min; (f) 6-nitro-2,2′-dimethylchromene epoxide: the column temperature was programmed from 80 to 200 °C with 4 °C min^{-1} and retained at 200 °C for 5 min, $t_{SS} = 30.3$ min, $t_{RR} = 30.8$ min.

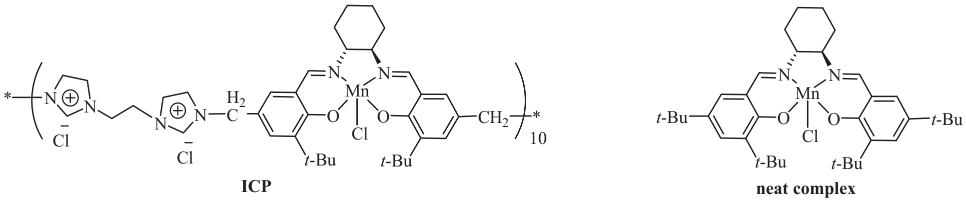

Chart 1. Structures of **ICP** and neat complex.

3. Results and discussion

3.1. Preparation of PICP-n (n = 3, 8, 12)

PEG is a fascinating phase transfer reagent with tunable solubility [22]. Catalyst containing the PEG moiety often behaves as a PTC for biphasic reaction and also can be facile recovered by solvent precipitation [33,34]. The inherent advantages encouraged us to introduce the PEG moiety into the framework of chiral salen Mn(III) complex to fabricate a reusable PTC of chiral salen Mn(III) complex for asymmetric epoxidation of unfunctionalized olefins in dichloromethane using NaClO as an oxidant. ILs derived from N,N-dialkylimidazolium are found to stabilize the chiral salen Mn(III) complex during the process of epoxidation and/or accelerate the reaction [9,25]. Therefore, PEG-modified imidazolium IL was chose to modify the chiral salen Mn(III) complex for the desirable fabrication. Given that increasing the number of active sites on catalyst may result in higher reactivity, we attempted to use PEG-modified imidazolium IL and chiral salen Mn(III) unit as the building blocks to prepare a ABAB-type polymeric matrix resemble PEG.

The synthesis route for the **PICP-*n*** (*n* = 3, 8, 12) was outlined in Scheme 1. At first, PEG-bridged di-imidazole with various length of PEG chain was obtained by nucleophilic substitution of chloride-terminated PEG with imidazolinium sodium salt under alkaline condition. Successive N-alkylation of the PEG-bridged di-imidazole with the chloromethyl groups (—CH_2Cl) at 5- and 5′-positions in (*R,R*′)-(N,N′-bis(3-*tert*-butyl-5-chloromethyl salicylidene)-1,2-cyclohexane diaminato) manganese(III) chloride resulted in the polymerization of chiral salen Mn(III) complex with PEG-bridged di-imidazole through forming imidazolinium-based IL, as shown in Scheme 1. PEG-based dicationic IL thus alternates with the chiral complex unit in the polymeric matrix, affording the **PICP-*n*** (*n* = 3, 8, 12) as brown and viscous liquid. For comparison, a PEG-free counterpart of **ICP**, in which chiral salen Mn(III) unit alternates with ethyl-based dicationic IL, was also prepared according to a preparation procedure similar to that of **PICP-*n***, except for the use of 1,2-dichloroethane instead of the chloride-terminated PEG during the preparation, as shown in Scheme 1.

Fig. 1 shows the solubility of PICP-*n* (*n* = 3, 8, 12) and ICP in water (Fig. 1A, 0.5 g sample in 5 ml water) and in dichloromethane (Fig. 1B, 0.5 g sample in 5 ml dichloromethane). As expected, all the PICP-*n* (*n* = 3, 8, 12) are soluble not only in dichloromethane (Fig. 1B, a–c), but also in water (Fig. 1A, a–c), at room temperature. The amphiphilic nature enables PICP-*n* to behave as efficient PTC in the water-dichloromethane biphasic reaction. Interestingly, although polymeric analog, the PEG-free counterpart of ICP is practically insoluble in water (Fig. 1A-d). We can thus speculate that the water-solubility of PICP-*n* is directly related with the PEG moiety. Actually, the water-solubility of catalyst decreases as the length of polyether chain increases (Fig. 1A-a vs A-b vs A-c). Whereas, the length of polyether chain does not have significant effect on the solubility of catalyst in dichloromethane (Fig. 1B-a vs B-b vs B-c). Notably, the PICP-*n* (*n* = 3, 8, 12) are almost insoluble in *n*-hexane or ether. It is suggested that the PTC of PICP-*n* (*n* = 3, 8, 12) could be recovered from the biphasic reaction by simple phase separation techniques via change of solvents.

3.2. Characterization of samples

3.2.1. FT-IR

The polymerization behavior of chiral salen Mn(III) complex unit with PEG-based dicationic IL in **PICP-*n*** (*n* = 3, 8, 12) was further confirmed by FT-IR analysis. Fig. 2 shows the FT-IR spectra of **PICP-*n*** (*n* = 3, 8, 12), as well as **ICP** and neat complex for comparison. Obviously, the FT-IR spectrum of neat complex shows the C—H vibrations (in the range of 2995–2750 cm^{-1}) associated with *t*-butyl groups and the C═C skeletal stretching vibrations (in the range of 1500–1250 cm^{-1}) associated with benzene rings in salen ligand. Furthermore, four characteristic vibration bands at around 1612, 1535, 569, and 413 cm^{-1} are also observed, which are associated with the stretching vibration modes of C═N, C—O, Mn—O, and Mn—N, respectively (Fig. 2a) [9,25,35]. While the characteristic bands appear as red shift from 1612, 1535, 569, and 413 cm^{-1} to 1618, 1543, 571 and 416 cm^{-1}, respectively, in the FT-IR spectra of **PICP-*n*** (*n* = 3, 8, 12), compared with those of neat complex (Fig. 2b-d vs 2a). It is mainly due to the electron-deficient substitutes of the imidazolium cations at the 5- and 5′-positions in salen ligands [36]. The presence of imidazolium IL moiety in the polymeric matrixes is also evident from the a newly formed band at 622 cm^{-1} associated with stretching vibration mode of C—N—C in imidazolium cation

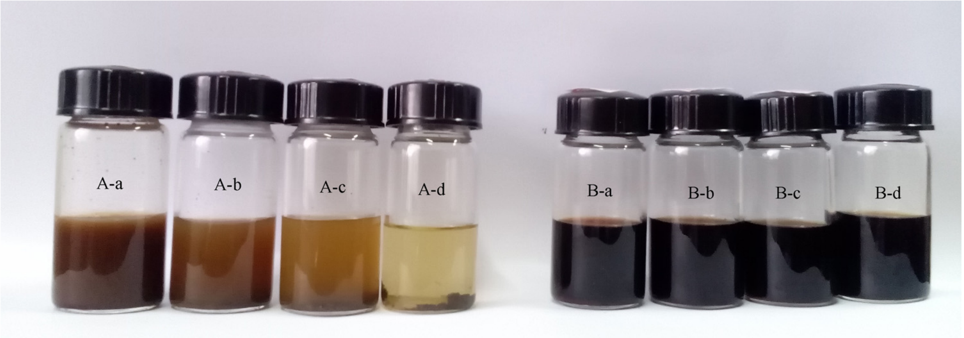

Fig. 1. Photographs of **PICP-3** (a), **PICP-8** (b), **PICP-12** (c) and **ICP** (d) in water (A) (0.5 g sample in 5 ml water) and in dichloromethane (B) (0.5 g sample in 5 ml dichloromethane).

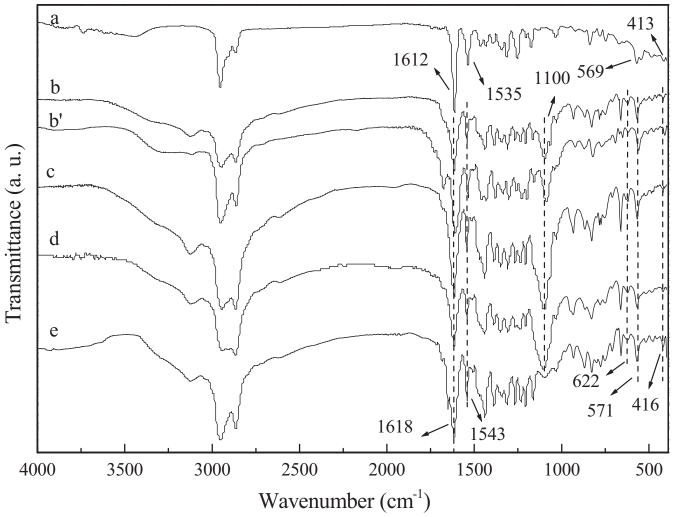

Fig. 2. FT-IR spectra of neat complex (a), **PICP-3** (b), **PICP-3** after seven runs (b'), **PICP-8** (c), **PICP-12** (d), and **ICP** (e).

(Fig. 2b-d) [9]. The results indicate the successfully bridging chiral salen Mn(III) unit with PEG moiety through the formation of imidazolium IL, as shown in Scheme 1. An additional distinct FT-IR band at around 1100 cm^{-1} attributable to C—O—C stretching vibration indicates the presence of PEG moiety in the polymers (Fig. 2b-d) [37]. It is the amphipathic PEG chain that responsible for the built-in phase transfer capability of **PICP-*n***. The FT-IR spectrum of **ICP** is similar to that of **PICP-*n*** (Fig. 2e vs 2b-d), except for the absence of the characteristic C—O—C stretching vibration. The difference is related to the absence of the PEG moiety in the framework of **ICP**, as shown in Chart 1.

3.2.2. UV–vis

UV–vis analysis provided more direct evidence for the polymerization through forming IL. Fig. 3 shows the UV–vis spectra of **PICP-*n*** (n = 3, 8, 12), **ICP** and neat complex. Obviously, neat complex exhibits the characteristic peaks at around 324, 427 and 515 nm, which is due to charge transfer transition of salen ligand, metal-to-ligand charge-transfer transition and *d*-*d* transition of complex, respectively [31,38]. As for the **PICP-*n*** (n = 3, 8, 12), the corresponding characteristic peaks shift to 317, 406 and 502 nm, respectively (Fig. 3a vs b-d). The blue shift of characteristic peaks should also be due to the electronic effect arisen from the electron-deficient imidazolium cations at the 5- and 5′-positions of salen ligand [25]. The PEG-free counterpart of **ICP** shows similar tendency in the UV–vis spectrum (Fig. 3e), as compared with **PICP-*n***, suggesting the similar active sites between **ICP** and **PICP-*n***. Therefore, PEG moiety interspersed in **PICP-*n*** does not change the electronic properties of active site for chiral salen Mn(III) complex.

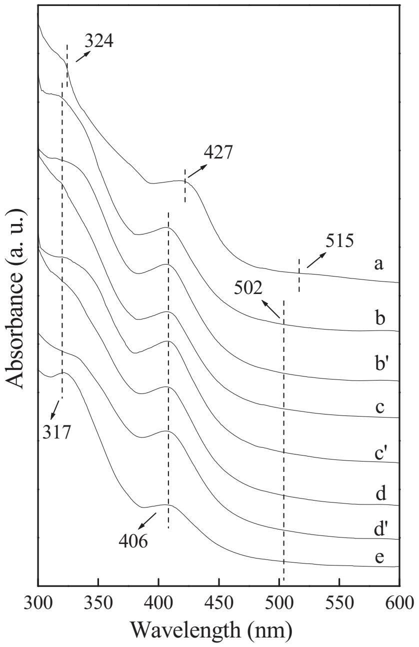

Fig. 3. UV–vis spectra of neat complex (a), fresh **PICP-3** (b), **PICP-3** after seven runs (b'), fresh **PICP-8** (c), **PICP-8** after seven runs (c'), fresh **PICP-12** (d), **PICP-12** after seven runs (d') and **ICP** (e).

3.2.3. Thermal analysis

Thermal analysis has been used to monitor the decomposition profiles of typical **PICP-8**, as well as neat complex and **ICP** for comparison. The results obtained are depicted in Fig. 4. Neat complex shows three distinct steps of weight loss in the combined TG–DTG curves, when heated from room temperature to 800 °C under air flow (Fig. 4A). The first loss in weight is centered at 110 °C, which is due to a release of chloride anions as hydrogen chloride. A second large weight loss appears at 216 °C, which is assigned to the cleavage of the *tert*-butyl groups [39]. The successive decomposition of residual salen ligand moieties occurs at 349 °C and extends up to 597 °C with the residue (ca. 12.3 wt%) amounting to manganese oxides. Fig. 4B displays the decomposition behavior of **PICP-8**, in which seven distinct steps of weight losses are observed. Interestingly, the release of chlorine anions in **PICP-8** exhibits two weight loss steps in combined TG-DTG curves, one at 122 °C and the other at 141 °C. As mentioned, the former weight loss is due to the release of chloride anions balanced with Mn(III) cation [39], while the second should be attributed to the loss of chloride counteranion in imidazolium IL moiety [40]. The third weight loss at 210 °C accounts for the cleavage of the *tert*-butyl groups, which is consistent with that of neat complex (Fig. 4B vs A). The fourth weight loss at 346 °C, which was absent in the combined TG-DTG curves of **ICP** (Fig. 4B vs D), is logical to assign to the decomposition of the polyether chain parts in **PICP-8**, since PEG-bridged di-imidazole shows similar major weight loss in the temperature range (Fig. 4B vs C). The fifth weight loss is at 397 °C, followed by an additional weight loss at 450 °C that extended up to ca. 501 °C. The two steps that were well distinguished in the DTG curve can be assigned to the successive cleavage of salen ligand moieties in **PICP-8**. Obviously, the corresponding decomposition temperature increases compared with that of neat complex (Fig. 4B vs A), because of the mutual stabilization of salen ligand part and the PEG-based IL moieties. It is indirect proof for the successful bridging chiral salen ligand with PEG-based IL moieties. Complete decomposition of the ILs moiety in **PICP-8** occurs at 625 °C, leaving non-removable residue belonged to the formed manganese oxide.

3.3. Catalytic performances

Asymmetric epoxidation of alkenes catalyzed by chiral salen Mn(III) complex using *aq.* NaClO as an oxidant have been extensively investigated in recent years because *aq.* NaClO is inexpensive, safe, and environmentally benign. Although high yield and enantioselectivity, the catalytic efficiency (in terms of TOF), are often limited by poor mass transfer in the water-dichloromethane biphasic system [15–19]. Complexes of **PICP-*n*** were designed as PTC for the asymmetric epoxidation of alkenes using *aq.* NaClO as an oxidant. We proposed that **PICP-*n*** with built-in phase transfer capacity could circumvent the mass transfer problem and enhance catalytic efficiency in the biphasic system. The results of the enantioselective epoxidation of different substrates at 0 °C,

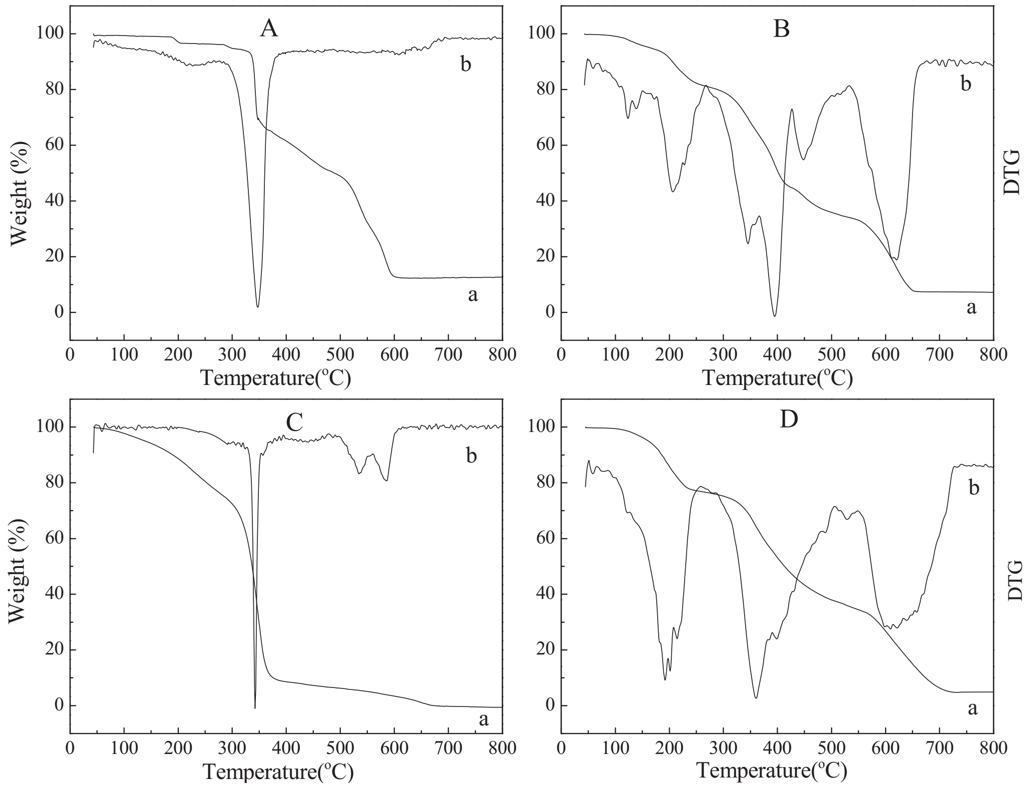

Fig. 4. TG-DTG curves of neat complex (A), **PICP-8** (B), PEG-bridged di-imidazole (C), and **ICP** (D) ((a) thermogravimetric curves; (b) differential thermogravimetric curves).

using **PICP-*n*** (n = 3, 8, 12) as catalysts and *aq.* NaClO as an oxidant in dichloromethane, are summarized in Table 1. To investigate the built-in phase transfer capability originated from PEG moiety, PEG-free counterpart (denoted as **ICP**) was prepared as a control catalyst by N-alkylation of ethyl-bridged di-imidazole with the chloromethyl groups (—CH$_2$Cl) at 5- and 5′-positions of chiral salen Mn(III) complex. Furthermore, the traditional chiral salen Mn(III) complex (as shown in Chart 1) was also employed for comparison.

As expected, neat chiral salen Mn(III) complex with limited water-solubility was less efficient in the water-dichloromethane biphasic system. Only 65% conversion of styrene was obtained within 60 min (Table 1, entry 1). Although still poor water-solubility, **ICP** offered higher conversion (74% of styrene) than neat complex (Table 1, entry 2 vs 1) due to the positive effect of imidazolium IL moieties on activating chiral salen Mn(III) complex [9,25] and/or some synergetic interaction between neighboring sites [26,27,41]. However, it was far less active than the catalysts of **PICP-*n*** (n = 3, 8, 12) (Table 1, entry 2 vs entries 3–5). Using *aq.* NaClO as an oxidant, the **PICP-*n*** gave excellent conversions (in the range of 82–96%) with 34% enantioselectivity (ee values) in the asymmetric epoxidation of styrene at 0 °C within 60 min (Table 1, entries 3–5). Enhanced catalytic efficiency over **PICP-*n*** should arise from the PEG chains interspersed in their framework. Amphipathic nature of PEG chain endows the **PICP-*n*** with desirable built-in phase transfer capacity in the water–dichloromethane biphasic reaction. Furthermore, the ether groups in PEG chain was reported to transport the real oxidant HClO from aqueous to organic phase through the formation of hydrogen bonds [25,41]. Mass transfer restriction associated with aqueous/organic biphasic system was thus well resolved. Slightly lower ee value (34%) upon **PICP-*n*** (n = 3, 8, 12) and **ICP** should be due to the variation of electronic property of the 5,5′-substituents in salen ligand (Table 1, entries 2–5). In most cases, complex bearing electron-deficient substituents, such as imidazolium cations, at the 5,5′-positions affords slight lower ee value [42]. The catalytic performance of **PICP-*n*** (n = 3, 8, 12) was also compared with that of other reported catalytic systems, such as chiral macrocyclic salen Mn(III) complex [15] and mesoporous silica supported chiral complexes [12] under similar conditions. As expected, **PICP-*n*** gave significantly higher catalytic activity (in terms of TOF value) than the reported catalysts either homogeneous (Table 1, entry entries 3–5 vs entry 6) or heterogeneous (Table 1, entries 3–5 vs 7–9). It is easy to understand that **PICP-*n*** with built-in phase transfer capacity circumvent mass transfer restriction associated with aqueous/organic biphasic system and give higher catalytic efficiency.

Furthermore, we noticed that various length of polyether chain in **PICP** affected the catalytic activity of corresponding complex in water–dichloromethane biphasic epoxidation. The conversion of styrene decreased with increasing the total length of polyether chain. **PICP-3** showed the highest catalytic activity, giving styrene epoxide in almost quantitative conversion (96%) with 34% ee value within 60 min (Table 1, entry 3). As the numbers of ethylene oxide unit in PEG chain increased from 3 to 8, and further increased to 12, the conversion decreased accordingly (Table 1, entries 3–5). In the case of **PICP-12**, only 82% conversion of styrene was obtained in the epoxidation (Table 1, entry 5). A possible explanation might be that the length of polyether chain directly affects the inherent phase transfer capability of corresponding complex, since the water-solubility of catalysts decrease as the total length of PEG chain increases, as shown in Fig. 1A (A-a vs A-b vs A-c). However, there is no change in enantioselectivity with lengthening PEG chain.

Remarkably enhanced catalytic efficiency over the **PICP-3** was also observed in the case of the α-methylstyrene, indene, 1,2-dihydronaphthalene, 6-cyano-2,2-dimethylchromene and 6-nitro-2,2-dimethylchromene, as shown by TOF in Table 1 (entries 12, 15, 18, 21 and 24). Notably high TOF values were obtained over **PICP-3** in the epoxidation of the substrates. The TOF values are

Table 1
Results of the enantioselective epoxidation of unfunctionalized olefins over different chiral salen Mn(III) complexes[a].

Entry	Catalyst	Substrate	Product	Conv.[b]/%	ee[b]/%	Yield[c]/%	TOF[d] $\times 10^{-3}$/s^{-1}
1	Neat complex			65	39	60	4.51
2	**ICP**			74	34	68	5.13
3	**PICP-3**			96	34	90	6.67
4	**PICP-8**			86	34	80	5.97
5	**PICP-12**	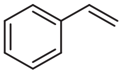	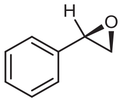 *R*	82	34	77	5.69
6	Polymer **1a**[e] Ref. [15]			99	33	95	1.83
7	CAT2-41[f] Ref. [12]			66	25	ns[g]	0.38
8	CAT2-48[f] Ref. [12]			79	31	ns[g]	0.46
9	CAT2-15[f] Ref. [12]			82	30	ns[g]	0.47
10	Neat complex			74	45	72	5.14
11	**ICP**	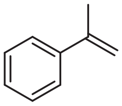	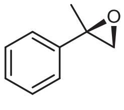 *R*	85	41	79	5.90
12	**PICP-3**			97	41	91	6.74
13	Neat complex			72	70	66	5.00
14	**ICP**	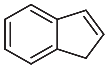	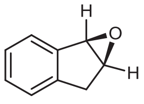 *1R, 2S*	78	67	71	5.42
15	**PICP-3**			93	67	86	6.46
16	Neat complex			66	80	61	4.58
17	**ICP**	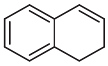	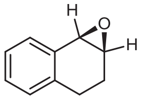 *1R, 2S*	73	77	67	5.07
18	**PICP-3**			93	77	87	6.46
19	Neat complex			56	95	49	3.89
20	**ICP**	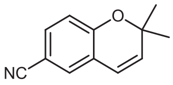	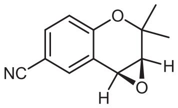 *3R, 4R*	62	92	56	4.31
21	**PICP-3**			91	93	85	6.32
22	Neat complex			56	95	50	3.89
23	**ICP**	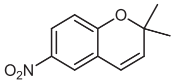	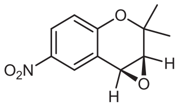 *3R, 4R*	63	93	59	4.38
24	**PICP-3**			91	93	84	6.32

[a] Catalyst (4 mol% of substrate, based on Mn ion content), substrate (0.5 mmol), pyridine *N*-oxide (1.0 mmol), NaClO (1.0 mmol, pH = 11.5, added in four equal parts), CH_2Cl_2 (2 ml), 60 min, 0 °C.

[b] Determined by GC.

[c] Isolated yields.

[d] TOF is calculated by the expression of [product]/[catalyst] × time (s^{-1}).

[e] Catalyst (5 mol% of substrate, based on Mn ion content), styrene (0.625 mmol), pyridine *N*-oxide (0.12 mmol), NaOCl (1.5 mmol, pH = 11.5, added in four equal parts), CH_2Cl_2 (1 ml), 3 h, 0 °C.

[f] Catalyst (2 mol% of substrate, based on Mn ion content), styrene (1 mmol), phenylpyridine *N*-oxide (0.38 mmol), NaOCl (2 mmol, pH = 11.5, added in four equal parts), CH_2Cl_2 (3 ml), 24 h, 0 °C.

[g] Not supplied.

significantly higher than those of **ICP** (Table 1, entry 12 vs 11, entry 15 vs 14, entry 18 vs 17, entry 21 vs 20, entry 24 vs 23), and also those of neat complex in corresponding epoxidations (Table 1, entry 12 vs 10, entry 15 vs 13, entry 18 vs 16, entry 21 vs 19, entry 24 vs 22). Excellent conversions (in the range of 91–97%) were obtained with all the alkenes used in this work but the highest chiral induction (93%) was observed for the electron deficient 6-cyano-2,2-dimethylchromene and 6-nitro-2,2-dimethylchromene (Table 1, entries 21 and 24). The relatively bulkier olefins, such as indene and 1,2-dihydronaphthalene, show the moderate ee values (67% and 77%, respectively) (Table 1, entries 15 and 18), while, the ee values were not encouraging in the case of the terminal-olefins, such as styrene and α-methylstyrene (Table 1, entries 3 and 12).

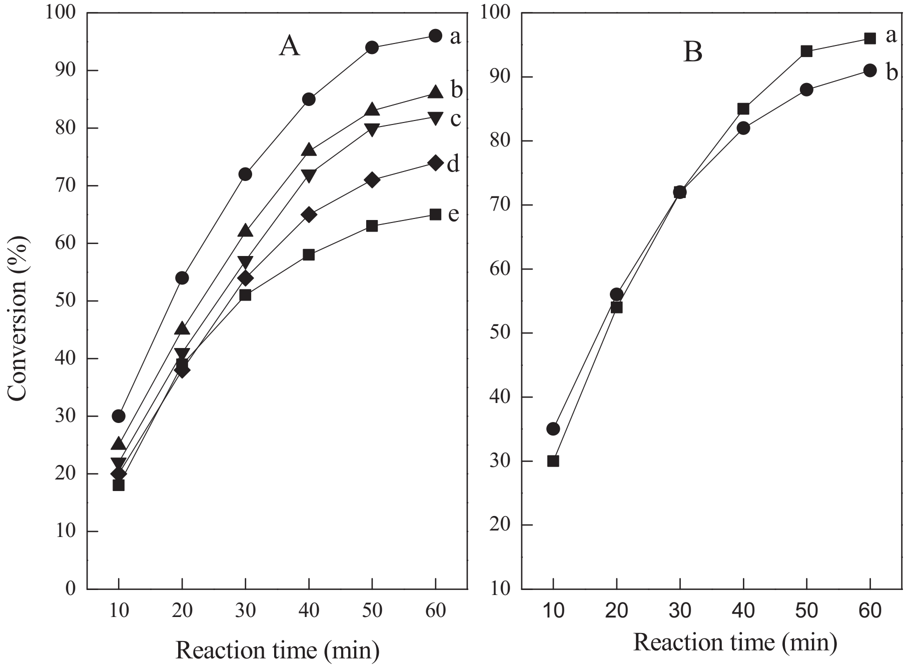

Fig. 5. The conversion vs reaction time plot for asymmetric epoxidation of styrene (A) catalyzed by **PICP-3** (a), **PICP-8** (b), **PICP-12** (c), **ICP** (d) and neat complex (e), and the conversion vs reaction time plot for **PICP-3** (B) with typical styrene (a) and 6-nitro-2,2-dimethylchromene (b) as substrates.

In order to understand the process of phase transfer catalysis in the aqueous/organic biphasic system, we have used kinetics to study the reaction rates of asymmetric epoxidation of styrene over the catalysts of neat complex, **ICP** and **PICP-*n*** ($n = 3, 8, 12$). The time-dependent plot of corresponding catalyst is shown in Fig. 5A. It is observed from the profile that conversion of styrene increased linearly up to 40 min, after which a significant increase is not observed. Therefore, the initial rate constants K_{obs} were determined from the data in this time range. Neat complex, **ICP**, **PICP-12**, **PICP-8** and **PICP-3** give K_{obs} values of 1.32, 1.51, 1.66, 1.70, and 1.83 M/min, respectively. The order of reaction rates over the all tested catalysts is thus as follows: **PICP-3** > **PICP-8** > **PICP-12** > **ICP**> neat complex, viewing from the kinetics point. The results demonstrate the built-in phase transfer capacity of **PICP-*n*** arisen from the PEG moiety. It circumvents the mass transfer restriction associated with aqueous/organic biphasic system, enhancing the reaction rate. And also, the inherent phase transfer decreased with increasing the total length of polyether chain of corresponding complex. Furthermore, the kinetic profiles for **PICP-3** with typical styrene and 6-nitro-2,2-dimethylchromene as substrates is also shown in Fig. 5B. It is observed from the profiles that conversion of substrates also increased linearly up to 40 min, after which a significant increase is not observed. Therefore, the initial rate constants K_{obs} were determined from the data in this time range. Epoxidation of styrene and 6-nitro-2,2-dimethylchromene over **PICP-3** give K_{obs} values of 1.83 and 1.57 M/min, respectively. Thus, the reaction rates of styrene is faster that that of 6-nitro-2,2-dimethylchromene, viewing from the kinetics point. The difference in reaction rates should be relevant to the mass transfer in reaction system. Actually, 6-nitro-2,2-dimethylchromene itself is solid and is insoluble in water.

Since the water-soluble **PICP-*n*** ($n = 3$, 8, 12) are selectively soluble in some organic solvents, various solvents should affect the built-in phase transfer capacity, and further the catalytic performance of catalyst in the asymmetric epoxidation of non-functionalized alkenes. Table 2 summarizes the results of comparative study of the enantioselective epoxidation of styrene over **PICP-3** in various solvents. As shown in Table 2, the epoxidation results indicated differences in catalytic activity and enantioselectivity depending on the solubility of catalyst, as well as the coordinative ability of solvent. **PICP-3** is difficultly soluble in *n*-hexane and ether, the problem associated with mass transfer is still encountered. Poor conversion and ee value were indeed obtained when the reaction was performed in *n*-hexane (22% of conversion with 14% ee value) or in ether (26% conversion with the 15% ee value) (Table 2, entries 1 and 2). If the catalyst can be dissolved completely in reaction medium, conversion and ee value should be enhanced. In the case of dichloromethane, 96% conversion with 34% ee value could be obtained within 60 min (Table 2, entry 3). However, the catalytic activity of **PICP-3** was not encouraging in methanol, acetone, and acetonitrile, although the catalyst can also be readily dissolved (Table 2, entries 4, 5, and 6). The principal explanation for this difference is that the solvent containing oxygen or nitrogen atom with lone electron pair can induce probably coordination with metal center of complex, suppressing the ability of the formation of the active oxygen transfer species (Mn(V)-oxo) in the epoxidation of styrene [9,25,43]. Notably, water-soluble **PICP-3** is also inactive in water. Only 35% conversion with 3% ee value was obtained in water (Table 2, entry 7). The lower activity is attributed to the limited solubility of styrene in the aqueous solution of the catalyst and oxidant, and the poor enantioselectivity is partially due to the solvation of water. The solvent effect on the catalytic performance of **PICP-3** also proved to be valid when 6-nitro-2,2-dimethylchromene (with higher product ee) was performed as the substrate (Table 2, entries 8–14). Therefore, dichloromethane is a suitable solvent, in which the catalyst behaves as the efficient PTC to smoothly catalyze the asymmetric epoxidation.

3.4. *Reusability*

Different from the traditional PTC, the catalysts of **PICP-*n*** ($n = 3$, 8, 12) not only efficiently accelerate the biphasic epoxidation, but also can be easily precipitated out from the reaction system by adding sufficient *n*-hexane to reaction mixture. The supernatant with the product was separated from catalyst by simple decantation. Recovered catalyst can be readily recycled by adding fresh reaction substrates.

Table 2
Results of asymmetric epoxidation of unfunctionalized olefins in different solvents over **PICP-3**[a].

Entry	Substrate	Solvent	Conv.[b]/%	*ee*[b]/%	Yield[c]/%	*TOF*[d] × 10^{-3}/s^{-1}
1		*n*-Hexane	22	14 (*R*)	17	1.53
2		Ether	26	15 (*R*)	20	1.81
3		Dichloromethane	96	34 (R)	90	6.67
4	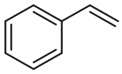	Methanol	72	12 (*R*)	68	5.00
5		Acetone	80	27 (*R*)	75	5.56
6		Acetonitrile	77	21 (*R*)	73	5.35
7		Water	35	3 (*R*)	30	2.43
8		*n*-Hexane	20	47 (*R*)	14	1.38
9		Ether	32	51 (*R*)	27	2.22
10		Dichloromethane	91	93 (*R*)	85	6.32
11	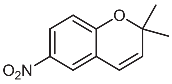	Methanol	67	39 (*R*)	62	4.65
12		Acetone	78	58 (*R*)	72	5.42
13		Acetonitrile	72	63 (*R*)	67	5.00
14		Water	41	12 (*R*)	37	2.85

[a] **PICP-3** (4 mol% of substrate, based on Mn ion content), styrene (0.5 mmol), pyridine *N*-oxide (1.0 mmol), NaClO (1.0 mmol, pH = 11.5, added in four equal parts), solvent (2 ml), 60 min, 0 °C.
[b] The same as Table 1.
[c] The same as Table 1.
[d] The same as Table 1.

Fig. 6 shows the results of the recovery and reusability of these catalysts in the asymmetric epoxidation of styrene using NaClO as an oxidant (Fig. 6A–C). To our delight, **PICP-*n*** (*n* = 3, 8, 12) could be reused up to seven times with no significant loss in yield and enantioselectivity of styrene epoxide. The leaching tests to the reaction medium were performed by directly determining the manganese content in supernatant via chemical analysis. No manganese was detected in the supernatant, which reveals negligible leaching loss of Mn species during the reaction. Furthermore, chemical analysis of the recovered catalysts gives manganese content (0.809, 0.692, and 0.738 mmol/g for recovered **PICP-3**, **PICP-8**, and **PICP-12**, respectively) almost identical to that of the corresponding fresh one (0.814, 0.695, and 0.741 mmol/g for fresh **PICP-3**, **PICP-8**, and **PICP-12**, respectively). Therefore, the efficient PTC of **PICP-n** is quite stable under the basic reaction condition (pH 11.5, NaClO buffer). Oxidative decomposition of chiral salen Mn(III) complex, a main reason for deactivation of the complex in basic epoxidation [44], did not occur during the reaction. Further evidence for the stability of catalysts was provided by UV–vis spectra. No significant changes of the catalysts took place even after reuse for seven times (Fig. 3b vs b', c vs c', d vs d'). Perfect stability of **PICP-*n*** (*n* = 3, 8, 12) was also proved by the reusability of typical **PICP-3** in asymmetric epoxidation of 6-nitro-2,2-dimethylchromene (Fig. 6D). Characterization of the recycled **PICP-3** (after seven runs) by FT-IR spectra shows no significant changes of the **PICP-3** even after reuse for seven times (Fig. 2 b vs b'). Manganese content of recycled

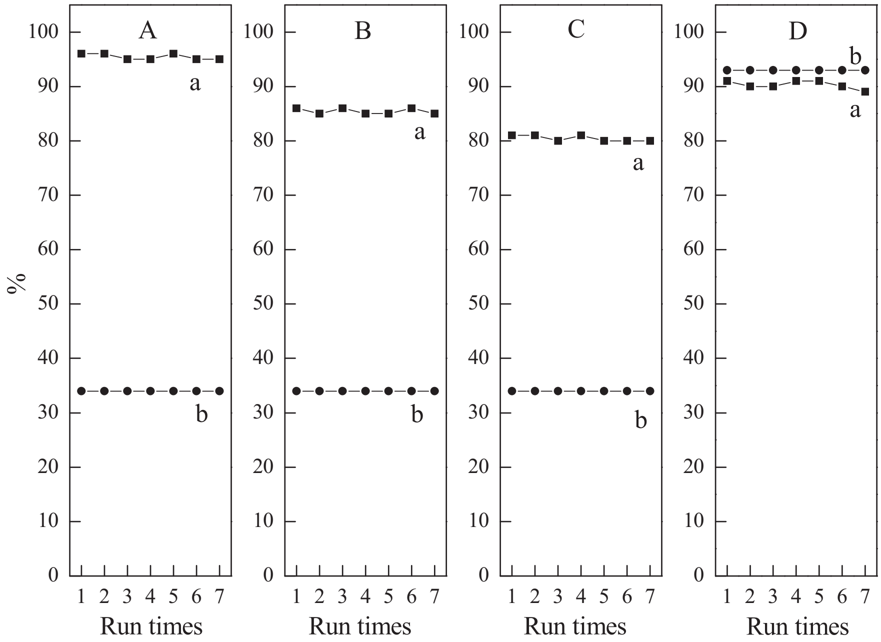

Fig. 6. Reuse of **PICP-3** (A), **PICP-8** (B) and **PICP-12** (C) in the asymmetric epoxiation of styrene, and reuse of **PICP-3** in the asymmetric epoxiation of 6-nitro-2,2-dimethylchromene (D) with *aq.* NaClO at 0 °C (a: conversion; b: ee value).

PICP-3 (0.811 mmol/g) determined by chemical analysis is also almost identical to that of the fresh one (0.814 mmol/g). The excellent stability of **PICP-*n*** in the reaction system should origin from mild reaction conditions and stable structure of the complex. Short reaction time (within 60 min) and low temperature (0 °C) used in our studies would prevent or at least slow catalyst degradation. More importantly, the possibility of formation of undesired inactive dimeric μ-oxo-manganese(IV) dimmers, the other cause for deactivation of the catalytic species, can be avoided because of the severe restriction of active site (site isolation) in the rigid one-dimension polymer framework [6,9]. Furthermore, the imidazolium IL linker moiety plays a positive effect on stabilizing the complex [9,25].

4. Conclusions

Chiral salen Mn(III) polymers (**PICP-*n*** (*n* = 3, 8, 12)), in which chiral salen Mn(III) unit was linked side by side through various PEG-based di-imidazolium IL bridge, were first prepared and acted as the phase transfer catalysts in enantioselective epoxidation of unfunctionalized olefins using *aq.* NaClO as an oxidant. Remarkable enhancement of reaction rate with notably high TOF values was observed over the **PICP-*n*** (*n* = 3, 8, 12), especially over **PICP-3**, in the water-dichloromethane biphasic system. Furthermore, the synthesized **PICP-*n*** (*n* = 3, 8, 12) is quite stable under the basic reaction condition (pH 11.5, NaClO buffer) and could be facilely recovered from the reaction system for efficient reuse. The built-in phase transfer capability, high catalytic efficiency, as well as prefect stability and reusability render this kind of complexes attractive in the enantioselective epoxidation of unfunctionalized olefins with *aq.* NaClO.

Acknowledgements

The project was financially supported by the National Natural Science Foundation of China (Grant Nos. 21476069, 21003044), the Scientific Research Fund of Hunan Provincial Education Department (13B072), the Program for Excellent Talents in Hunan Normal University, the Program for Science and Technology Innovative Research Team in Higher Educational Institutions of Hunan Province.

References

[1] M. Tokunaga, J.F. Larrow, F. Kakiuchi, E.N. Jacobsen, Science 277 (1997) 936–938.
[2] H. Yang, L. Zhang, W. Su, Q. Yang, C. Li, J. Catal. 248 (2007) 204–212.
[3] O.A. Wong, Y. Shi, Chem. Rev. 108 (2008) 3958–3987.
[4] W. Zhang, J.L. Loebach, S.R. Wilson, E.N. Jacobsen, J. Am. Chem. Soc. 112 (1990) 2801–2803.
[5] S. Chang, J.M. Galvin, E.N. Jacobsen, J. Am. Chem. Soc. 116 (1994) 6937–6938.
[6] Q. Xia, H. Ge, C. Ye, Z. Liu, K. Su, Chem. Rev. 105 (2005) 1603–1662.
[7] C. Baleizão, H. Garcia, Chem. Rev. 106 (2006) 3987–4043.
[8] H. Zhang, Y. Zhang, C. Li, J. Catal. 238 (2006) 369–381.
[9] R. Tan, D. Yin, N. Yu, H. Zhao, D. Yin, J. Catal. 263 (2009) 284–291.
[10] O.Y. Lyakin, R.V. Ottenbacher, K.P. Bryliakov, E.P. Talsi, ACS Catal. 2 (2012) 1196–1202.
[11] J. Huang, X. Fu, C. Wang, H. Zhang, Q. Miao, Microporous Mesoporous Mater. 153 (2012) 294–301.
[12] R. Ji, K. Yu, L. Lou, S. Liu, J. Mol. Catal. A 378 (2013) 7–16.
[13] R.V. Ottenbacher, D.G. Samsonenko, E.P. Talsi, K.P. Bryliakov, ACS Catal. 4 (2014) 1599–1606.
[14] L. Ma, F. Su, X. Zhang, D. Song, Y. Guo, J. Hu, Microporous Mesoporous Mater. 184 (2014) 37–46.
[15] N.Ch. Maity, S.H.R. Abdi, R.I. Kureshy, N.H. Khan, E. Suresh, G.P. Dangi, J. Catal. 277 (2011) 123–127.
[16] B.I. Kuźniarska, C. Pereira, A.P. Carvalho, J. Pires, C. Freire, Appl. Clay Sci. 53 (2011) 195–203.
[17] Z. Liu, X. Fu, X. Hu, Q. Miao, J. Organomet. Chem. 713 (2012) 157–162.
[18] R.I. Kureshy, T. Roy, N.H. Khan, S.H.R. Abdi, A. Sadhukhan, H.C. Bajaj, J. Catal. 286 (2012) 41–45.
[19] Y. Zhang, Q. Zhou, W. Ma, J. Zhao, Catal. Commun. 45 (2014) 114–117.
[20] R.I. Kureshy, N.H. Khan, S.H.R. Abdi, S.T. Patel, P.K. Iyer, P.S. Subramanian, R.S. Jasra, J. Catal. 209 (2002) 99–104.
[21] B. Bahramian, V. Mirkhani, M. Moghadam, S. Tangestaninejad, Appl. Catal. A 301 (2006) 169–175.
[22] J. Chen, S.K. Spear, J.G. Huddleston, R.D. Rogers, Green Chem. 7 (2005) 64–82.
[23] X. Wang, L. Yin, T. Yang, Y. Wang, Tetrahedron: Asymmetry 18 (2007) 108–114.
[24] S. Paul, A.R. Das, Tetrahedron Lett. 54 (2013) 1149–1154.
[25] R. Luo, R. Tan, Z. Peng, W. Zheng, Y. Kong, D. Yin, J. Catal. 287 (2012) 170–177.
[26] R.I. Kureshy, N.H. Khan, S.H.R. Abdi, S.T. Patel, R.S. Jasra, Tetrahedron Lett. 42 (2001) 2915–2918.
[27] X. Liu, N. Tang, W. Liu, M. Tan, J. Mol. Catal. A 212 (2004) 353–358.
[28] Y. Xu, Y. Bai, J. Peng, J. Li, W. Xiao, G. Lai, J. Organomet. Chem. 765 (2014) 59–63.
[29] D. Bell, M.R. Davies, G.R. Green, I.S. Mann, Synthesis 6 (1995) 707–712.
[30] J.F. Larrow, E.N. Jacobsen, Y. Gao, Y.P. Hong, X.Y. Nie, C.M. Zepp, J. Org. Chem. 59 (1994) 1939–1942.
[31] L. Lou, K. Yu, F. Ding, X. Peng, M. Dong, C. Zhang, S. Liu, J. Catal. 249 (2007) 102–110.
[32] H. Ren, Y. Tian, H. Liang, The Handbook of Analytical Chemistry, Chemical Industry Press, Beijing, 1997, p. 559.
[33] F. Alonso, M. Yus, ACS Catal. 2 (2012) 1441–1451.
[34] M.R. Nabid, Y. Bide, Appl. Catal. A 469 (2014) 183–190.
[35] B.M. Choudary, T. Ramani, H. Maheswaran, L. Prashant, K.V.S. Ranganath, K.V. Kumar, Adv. Synth. Catal. 348 (2006) 493–498.
[36] J. Zou, L. Wang, R. Zeng, Structure Analysis of Organic Compounds, Science Press, Beijing, 2005, p. 48.
[37] H. Zhi, C. Lü, Q. Zhang, J. Luo, Chem. Commun. (2009) 2878–2880.
[38] F. Bigi, L. Moroni, R. Maggi, G. Sartori, Chem. Commun. (2002) 716–717.
[39] L. Frunza, H. Kosslick, H. Landmesser, E. Hijft, R. Fricke, J. Mol. Catal. A 123 (1997) 179–187.
[40] Y. Kong, R. Tan, L. Zhao, D. Yin, Green Chem. 15 (2013) 2422–2433.
[41] Y. Sun, N. Tang, J. Mol. Catal. A 255 (2006) 171–179.
[42] M. Palucki, N.S. Finney, P.J. Pospisil, M.L. Guler, T. Ishida, E.N. Jacobsen, J. Am. Chem. Soc. 120 (1998) 948–954.
[43] B. Gong, X. Fu, J. Chen, Y. Li, X. Zou, X. Tu, P. Ding, L. Ma, J. Catal. 262 (2009) 9–17.
[44] Z. Xu, X. Ma, Y. Ma, Q. Wang, J. Zhou, Catal. Commun. 10 (2009) 1261–1266.